Inferior Vena Cava Anomalies and Pathologies

Poojary Shweta Raviraj[1] Venkataswamy Chandana[2] Hagalahalli Nagarajegowda Pradeep[2] Chakenahalli Puttaraj Nanjaraj[2]

[1] Department of Radiology, JSS Medical College, Mysore, Karnataka, India
[2] Department of Radiology, Mysore Medical College and Research Institute, Mysore, Karnataka, India

Address for correspondence Venkataswamy Chandana, MBBS, MD, Department of Radiology, Mysore Medical College and Research Institute, Mysore 570001, Karnataka, India (e-mail: chandureddy.v79@gmai.com).

J Gastrointestinal Abdominal Radiol ISGAR 2023;6:21–31.

Abstract

Wide array of anatomical variations and pathologies affect the inferior vena cava (IVC). Multidetector computed tomography remains the most important modality to diagnose and evaluate the extent of involvement. The congenital variations such as duplication, anomalous course of renal veins, azygos continuation of IVC, etc., remain clinically indolent and are detected incidentally in abdominal imaging. This article describes the various congenital variants which include abnormalities in drainage, failure of development, and regression of the IVC. This article also highlights the important pathological conditions such as Budd–Chiari syndrome, primary and secondary neoplasms of the IVC, bland thrombosis, and retrograde opacification of the IVC.

Keywords

- inferior vena cava
- MDCT
- anatomical variations

Introduction

Inferior vena cava (IVC) is part of the systemic venous drainage of human body draining the abdomen, lower trunk, pelvis, and lower limbs. Multiple modalities are used in the evaluation of IVC including conventional venography, color Doppler imaging, multidetector computed tomography (MDCT), and magnetic resonance imaging.

Owing to the higher spatial resolution, multiplanar reconstruction, three-dimensional volumetric rendering, and being faster, MDCT plays an important role in assessing the anatomic variants and pathologies affecting the IVC. The ability to reconstruct high-resolution images in coronal and sagittal planes, aids in the surgical and interventional management of the IVC pathologies.

The main aim of this pictorial essay is to provide the practicing radiologist all the information required in a brief and concise manner regarding the identification of the conditions revolving around the often ignored entity, the IVC (►**Table 1**).

It mainly helps the radiologists to increase their knowledge of congenital and pathological processes which affect IVC. As many of the congenital anomalies are detected incidentally, it is important for the radiologist to correctly identify and classify these congenital anomalies. Identification of Budd–Chiari syndrome, differentiating primary IVC neoplasm from secondary tumoral infiltration, bland versus tumor thrombosis, all these relevant critical information helps the radiologist to guide the clinician for appropriate treatment planning. As these entities have significant clinical implications it is important to be aware of all these conditions to avoid diagnostic pitfalls.

Normal Anatomy and Development

IVC is divided into suprahepatic, intrahepatic, and infrahepatic parts. Infrahepatic part is further divided into suprarenal, renal, and infrarenal parts. IVC is derived from the three

article published online
December 21, 2022

DOI https://doi.org/10.1055/s-0042-1758129.
ISSN 2581-9933.

Thieme Medical and Scientific Publishers Pvt. Ltd., A-12, 2nd Floor, Sector 2, Noida-201301 UP, India

Table 1 Classification of IVC anomalies and pathologies

Anatomic variants
Abnormal drainage
Portal vein draining into IVC—Abernethy malformation
Pulmonary veins draining into IVC–Scimitar syndrome
Failure of development
Interruption of IVC
Failure of regression
Duplication of IVC
Circumaortic left renal vein
Others
Retrocaval ureter
Retroaortic left renal vein
IVC thrombosis
Bland thrombosis
Tumor thrombosis
Budd–Chiari syndrome
Primary neoplasm of the IVC
Retrograde opacification of the IVC

Abbreviation: IVC, inferior vena cava.

paired veins, namely, posterior cardinal, subcardinal, and supracardinal veins.

The three paired veins are described as:

- Subcardinal veins (blue in ►**Fig. 1**) receive the veins from the developing kidneys. Cranially and caudally they communicate with the posterior cardinal veins. The two subcardinals are connected by a transverse inter-subcardinal anastomosis at the level of the renal veins (►**Fig. 1**). The cranial part of the right subcardinal vein also connects with the right hepatocardiac channel (purple in ►**Fig. 1**).
- Supracardinal veins (pink in ►**Fig. 1**) communicate cranially and caudally with posterior cardinal veins. They also communicate with the subcardinal veins through anastomoses which join the subcardinals just below the renal veins (►**Fig. 1**).
- Posterior cardinal vein (green in ►**Fig. 1**) near their caudal ends receive the veins of the lower limb bud (external iliac) and of the pelvis (internal iliac). The caudal ends of the two posterior cardinal veins become interconnected by a transverse anastomosis.

Many parts of these longitudinal venous channels disappear.[1]

The veins that remain give rise to the IVC as follows in caudal to cranial sequence (►**Fig. 1**):

- Lowest part of the right posterior cardinal vein.
- Lower part of the right supracardinal vein.
- Right supracardinal-subcardinal anastomosis.
- Right subcardinal vein.
- Subcardinal-hepatocardiac anastomosis.
- Right hepatocardiac channel.

Anatomic Variants

Abnormal Drainage

Abnormal Drainage of Portal Vein into IVC: Abernethy Malformation

Abernethy malformation is a condition where there is an abnormal communication between portal and systemic circulation. In type 1 congenital extrahepatic portosystemic shunt (CEPS), there is complete drainage of portal blood into the systemic circulation via formation of an end-to-side shunt, with absent intrahepatic branches of portal vein. Type 1 shunts are further classified into those in which the splenic vein (SV) and superior mesenteric vein (SMV) drain separately into a systemic circulation (type 1a) and those in which the SV and SMV form a common trunk together and drain into systemic vein (type 1b) (►**Fig. 2**). In type 2 CEPS, the intrahepatic portal vein is present, but via a side-to-side shunt some of the portal flow is diverted into a systemic circulation.[2]

Pulmonary Veins Draining into IVC: Scimitar Syndrome

Scimitar syndrome is a rare congenital anomaly with partial anomalous pulmonary venous return. It comprises of hypoplasia of right lung, cardiac dextroposition, and pulmonary

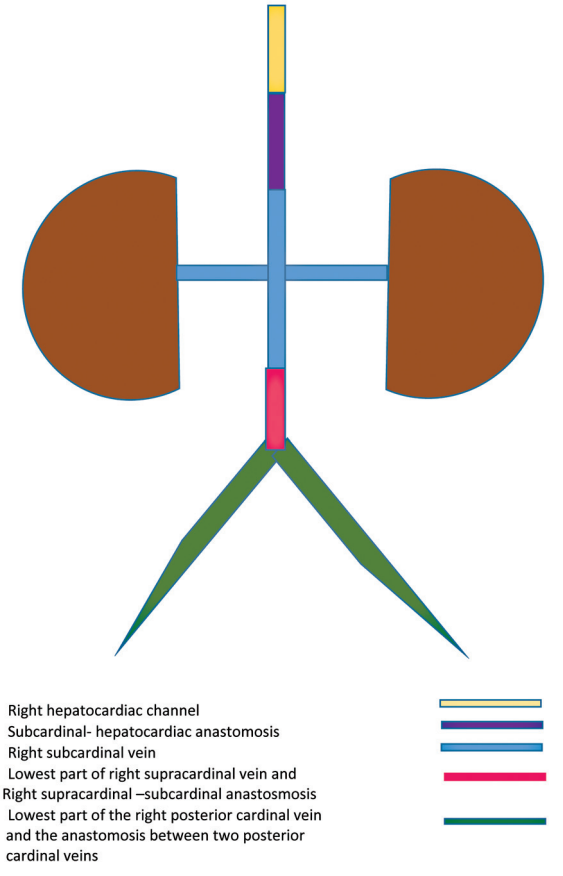

Fig. 1 Schematic diagram showing the embryology of inferior vena cava (IVC) development with color-coded annotations of the embryological vessels.

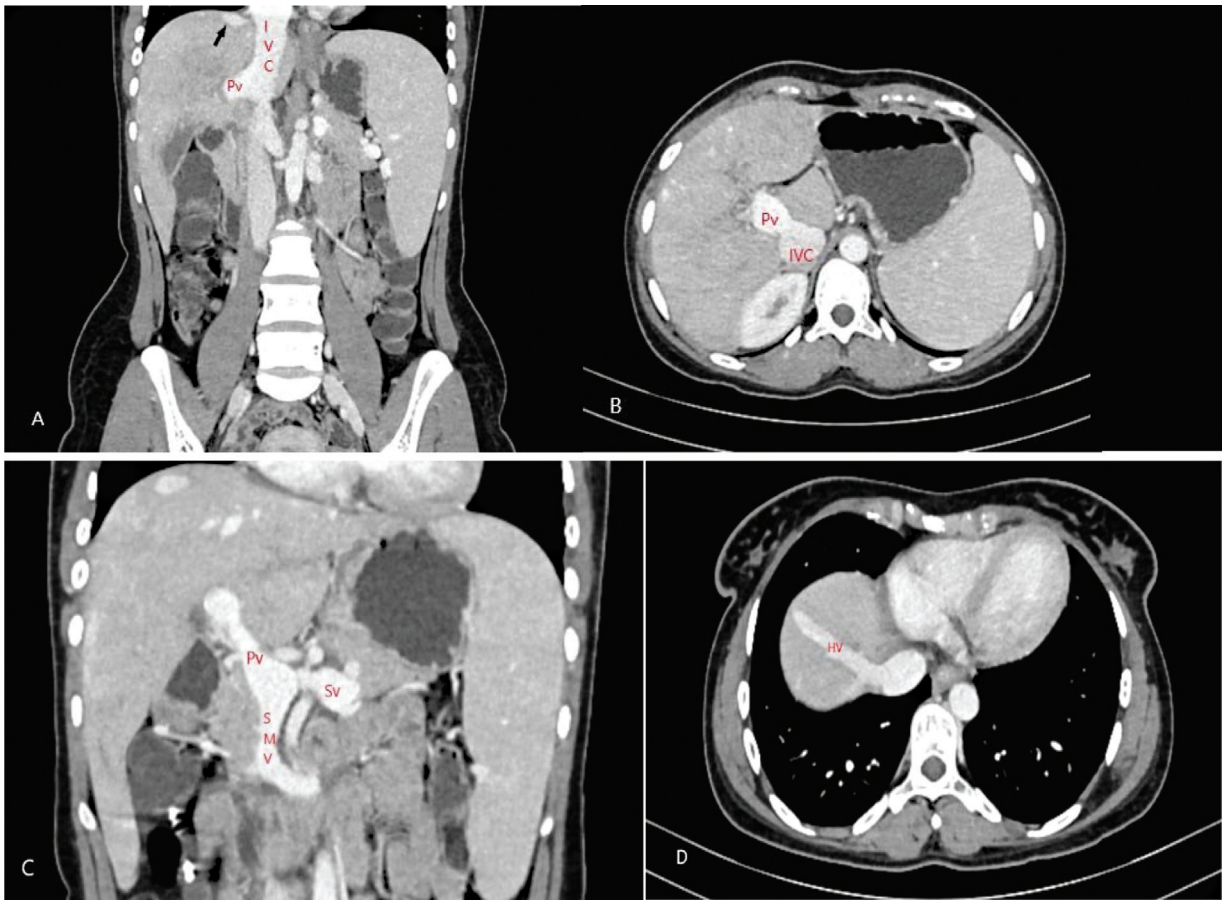

Fig. 2 Type 1b Abernethy malformation with an end-to-side congenital portosystemic anastomosis. (**A**) Coronal reformatted, postintravenous contrast computed tomography (CT) image and (**B**) axial intravenous contrast-enhanced CT image (venous phase) showing PV draining directly into the intrahepatic IVC. Hepatic veins (black arrow) draining into the IVC. (**C**) Coronal reformatted, postintravenous contrast CT image showing SV and SMV forming extrahepatic portal trunk (PV). (**D**) Axial intravenous contrast-enhanced CT image (venous phase) showing HV draining into the IVC. PV, portal vein; IVC, inferior vena cava; SV, splenic vein; HV, hepatic vein; SMV, superior mesenteric vein.

drainage of right lung into IVC[3] (►**Fig. 3**). The scimitar vein drains the entire right lung in two-thirds of the cases, whereas in the rest one-third only the lower portion of the right lung is drained by the vein.[4]

Failure of Development

Interruption of IVC

Infrahepatic interruption of the IVC with azygos continuation is a rare entity seen in asymptomatic individuals and also seen in patients with congenital heart disease[5] (►**Fig. 4**). It is a rare congenital abnormality where there is interruption of IVC below the hepatic veins and the lower limb veins drain via the azygos system into superior vena cava, whereas the drainage of hepatic veins is directly into the right atrium.[6]

Failure of Regression

Duplication of IVC

Persistence of right and left supracardinal vein results in duplication of IVC[7] (►**Fig. 5**). The duplicated left IVC joins the left renal vein, which in turn drains into the right IVC by crossing the midline. The incidence of double IVC is 0.2 to 3.0%.[8] The condition is often incidentally detected on diagnostic imaging. In certain situations it can be misdiagnosed as retroperitoneal lymphadenopathy.

Circumaortic Left Renal Vein

Developmental anomaly where two veins arise from the left renal vein surrounding the aorta. The ventral branch courses between the superior mesenteric artery and aorta draining into the IVC. The dorsal branch courses between the vertebral column and aorta draining into the IVC[9] (►**Fig. 6**). Recognition of this entity is essential as it often results in hematuria, proteinuria, and massive hemorrhage during surgery.[10]

Others

Retrocaval Ureter

Persistence of the right posterior cardinal vein as the renal segment of the IVC results in this anomaly. It is an abnormal relation between the ureter and the IVC where the ureter courses behind the IVC forming an S trajectory and further continues medial to it resuming the normal course[11] (►**Fig. 7**). Retrocaval ureter is more prone for stasis and

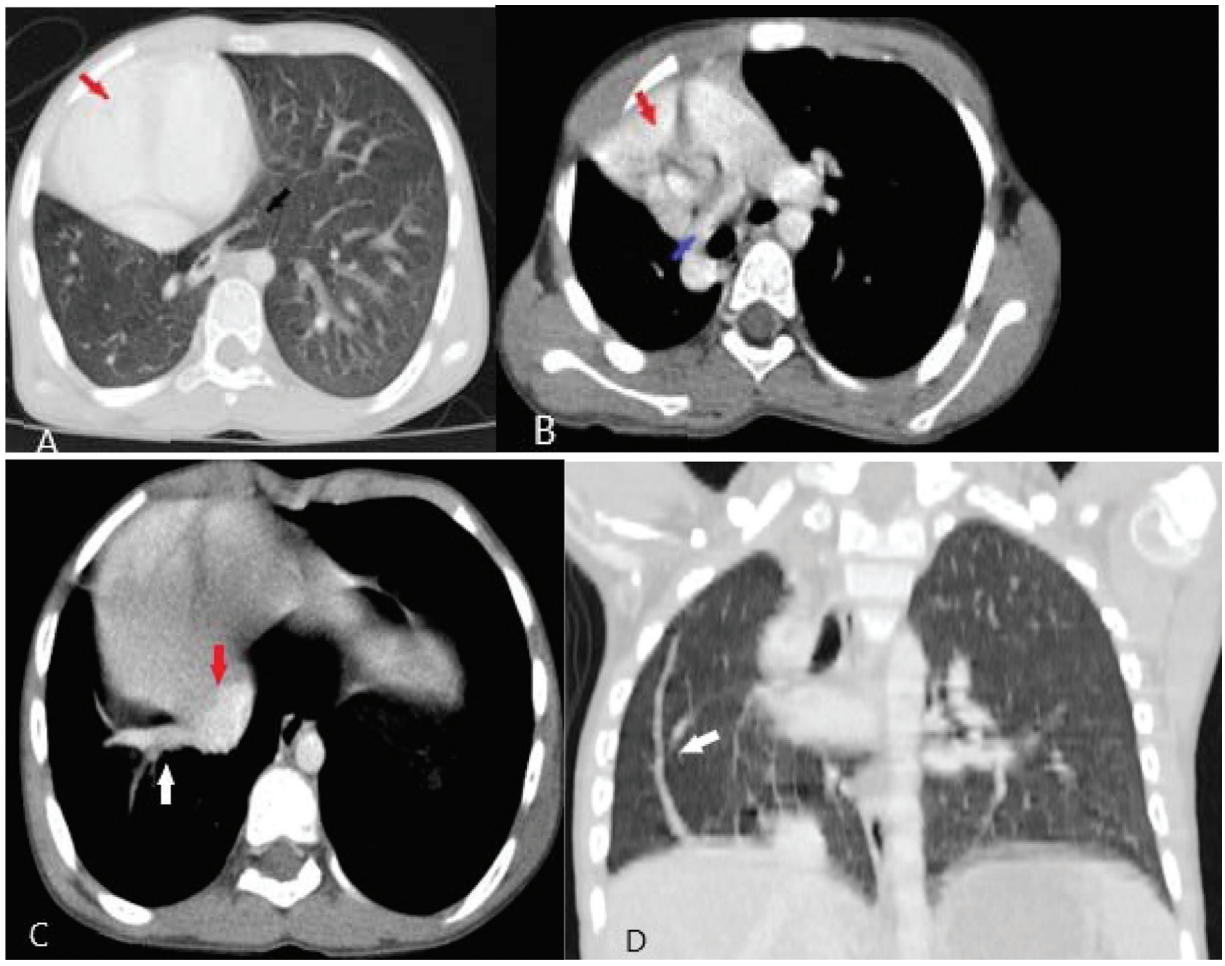

Fig. 3 (**A**) Axial postintravenous contrast computed tomography (CT) image (lung window) showing horse shoe lung (black arrow) and dextroposition of cardia (red arrow). (**B**) Axial intravenous contrast-enhanced CT image (venous phase), showing dextroposition of cardia (red arrow) and hypoplastic right pulmonary artery (blue arrow). (**C**) Axial intravenous contrast-enhanced CT image (venous phase), showing anomalous pulmonary vein (white arrow) draining the hypoplastic right lung into inferior vena cava (IVC) (red arrow) above the diaphragm. (**D**) Coronal reformatted, contrast CT image (lung window) shows curved anomalous pulmonary vein giving Turkish sword appearance. IVC, inferior vena cava.

calculi formation leading to hematuria. Other manifestations include cystitis, varicocele, and enuresis[12]

Retroaortic Left Renal Vein

A retroaortic left renal vein is located between the aorta and the vertebra, draining in to the IVC.[9] Although encountered in asymptomatic patients, this anomaly is of prime concern, when a left renal surgery is planned. Failure to recognize these anomalies may lead to severe hemorrhage and severe renal damage[13] (►**Fig. 8**). Compression of the retroaortic left renal vein between the aorta and the vertebra is known to be the cause of urological problems such as hematuria, varicocele, and pelviureteric junction obstruction.[14]

IVC Thrombosis

Bland Thrombus

Bland thrombus results from sluggish blood flow. Risk factors include hypercoagulable state, venous stasis, malignancies, and local compression which increase the likelihood of clot formation (►**Fig. 9**). Absence of intrathrombus enhancement in MDCT is highly indicative of bland thrombus. It requires thrombolytic and anticoagulant therapy.[15]

Tumor Thrombus

Tumor thrombus in cancer patients plays an important role in deciding the treatment outcome (►**Fig. 10**). Tumor thrombus in MDCT is characterized by expansion of the vessel lumen, contrast enhancement, and demonstration of contiguity of the thrombus with the mass. Renal cell carcinoma, adrenal cortical carcinoma, hepatocellular carcinoma, transitional cell carcinoma, and Wilms' tumor are few of the common secondary neoplasms involving the IVC.[16]

Budd–Chiari Syndrome

Budd–Chiari syndrome is a condition primarily seen in Asian countries characterized by partial or complete hepatic venous outflow obstruction (►**Fig. 11**). This obstruction can be at any level varying from the small hepatic veins to the junction of the IVC with the right atrium. This definition excludes hepatic outflow obstruction secondary

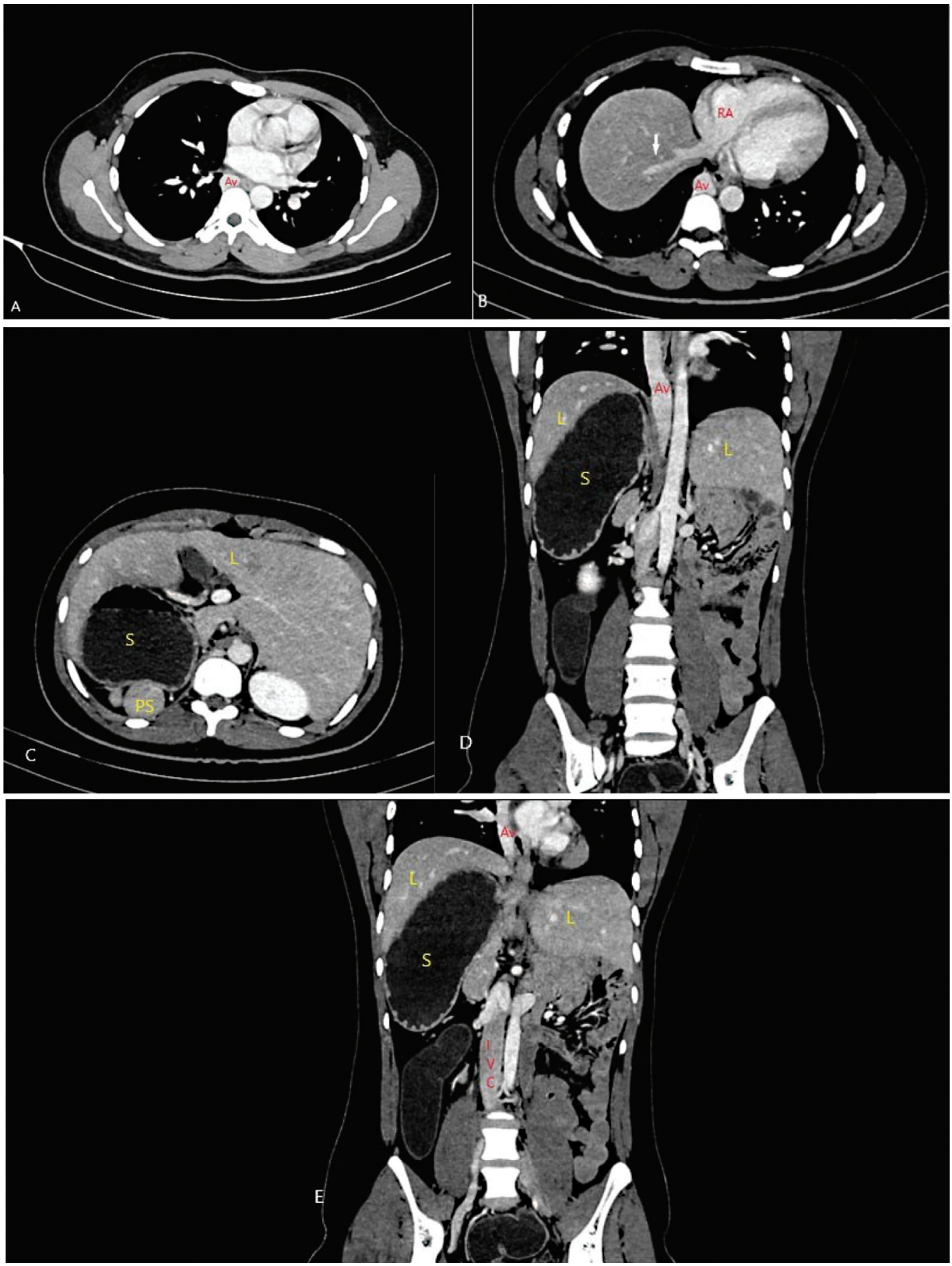

Fig. 4 (**A** and **B**) Axial postintravenous contrast computed tomography (CT) image (venous phase) showing the dilated Av and hepatic veins (white arrow) directly draining into the RA. (**C**) Axial intravenous contrast-enhanced CT image (venous phase), showing midline liver (L), right-sided stomach (S), and polysplenia (PS). (**D** and **E**) Coronal reformatted, intravenous contrast-enhanced CT image (venous phase), showing infrahepatic IVC continuing as dilated Av. Associated midline liver (L) and right-sided stomach (S). Av, azygos vein; IVC, inferior vena cava; RA, right atrium; L, liver; S, stomach; PS, polysplenia.

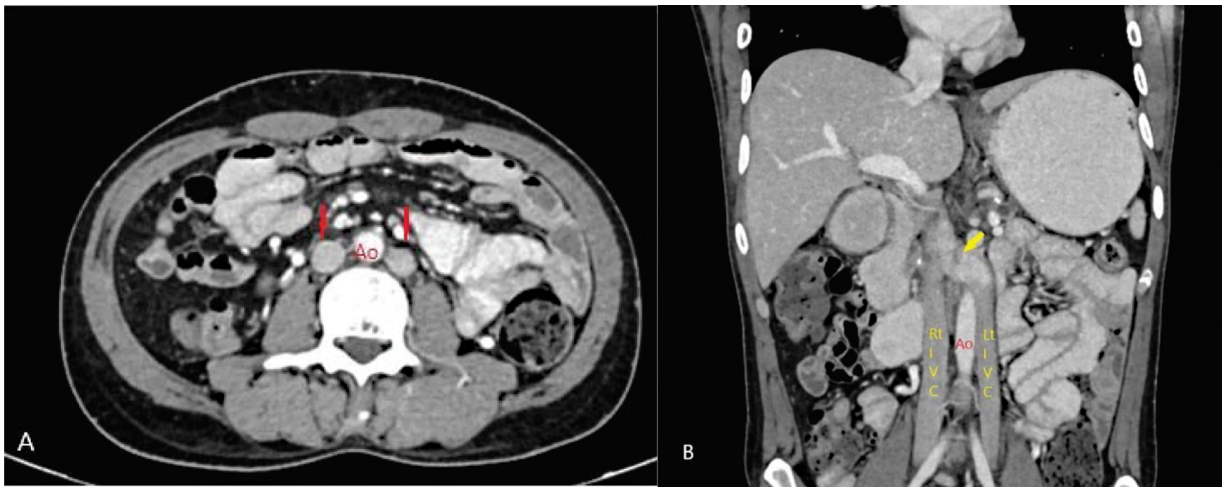

Fig. 5 (**A**) Axial postintravenous contrast computed tomography (CT) image (venous phase) showing double IVC (red arrows) below the renal veins on either side of the Ao. (**B**) Coronal reformatted, intravenous contrast-enhanced CT image (venous phase), showing the left IVC joining the right IVC coursing anterior to Ao (yellow arrow). IVC, inferior vena cava; Ao, aorta.

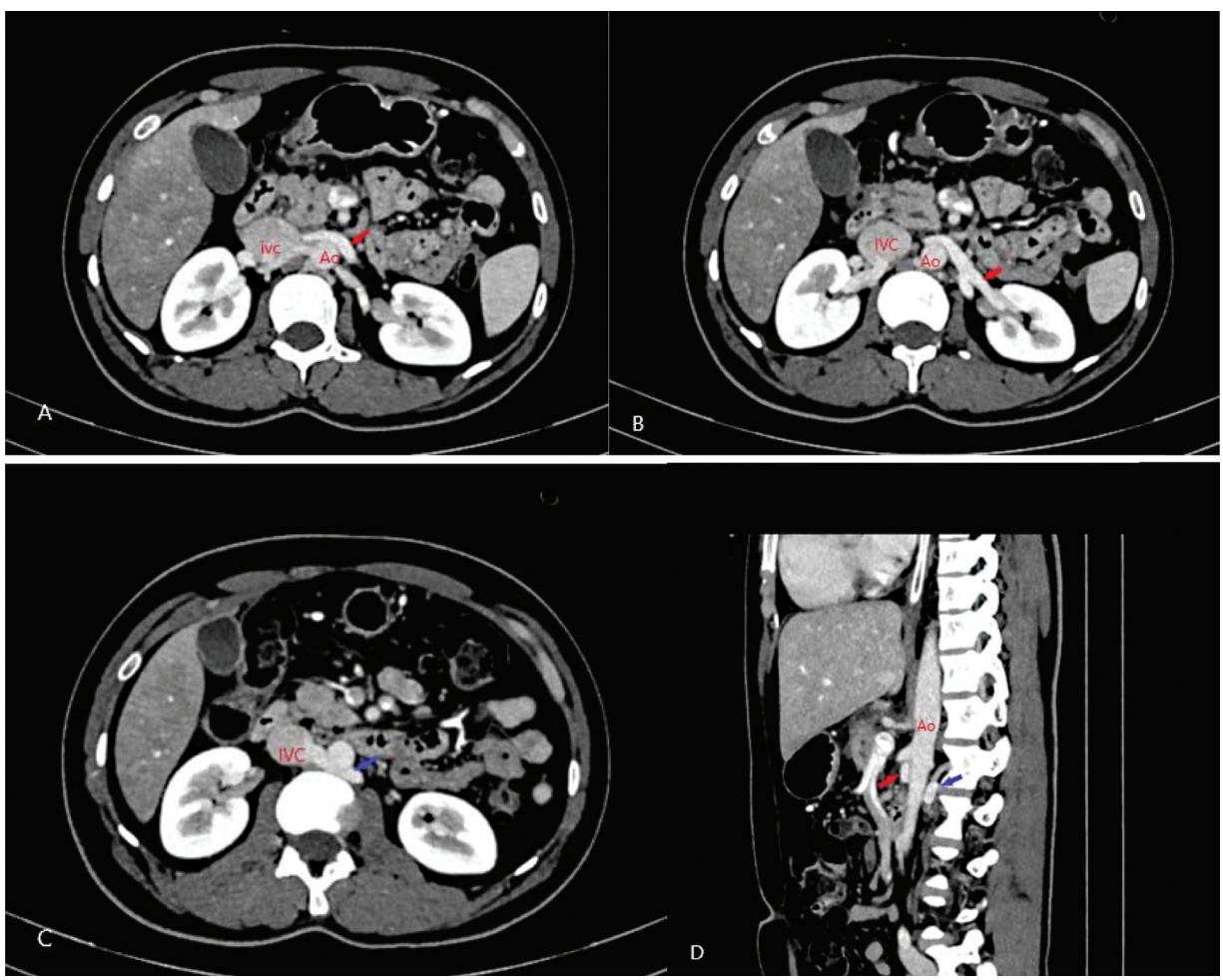

Fig. 6 (**A** and **B**) Axial postintravenous contrast computed tomography (CT) image (venous phase) showing the ventral branch of the left renal vein (red arrow) running between the aorta and the superior mesenteric artery, draining into the inferior vena cava (IVC). (**C**) Axial intravenous contrast-enhanced CT image (venous phase), showing the dorsal branch of the left renal vein (blue arrow). (**D**) Sagittal reformatted, intravenous contrast-enhanced CT image (venous phase), showing ventral (red arrow) and dorsal branches (blue arrow) of the left renal vein, surrounding the aorta.

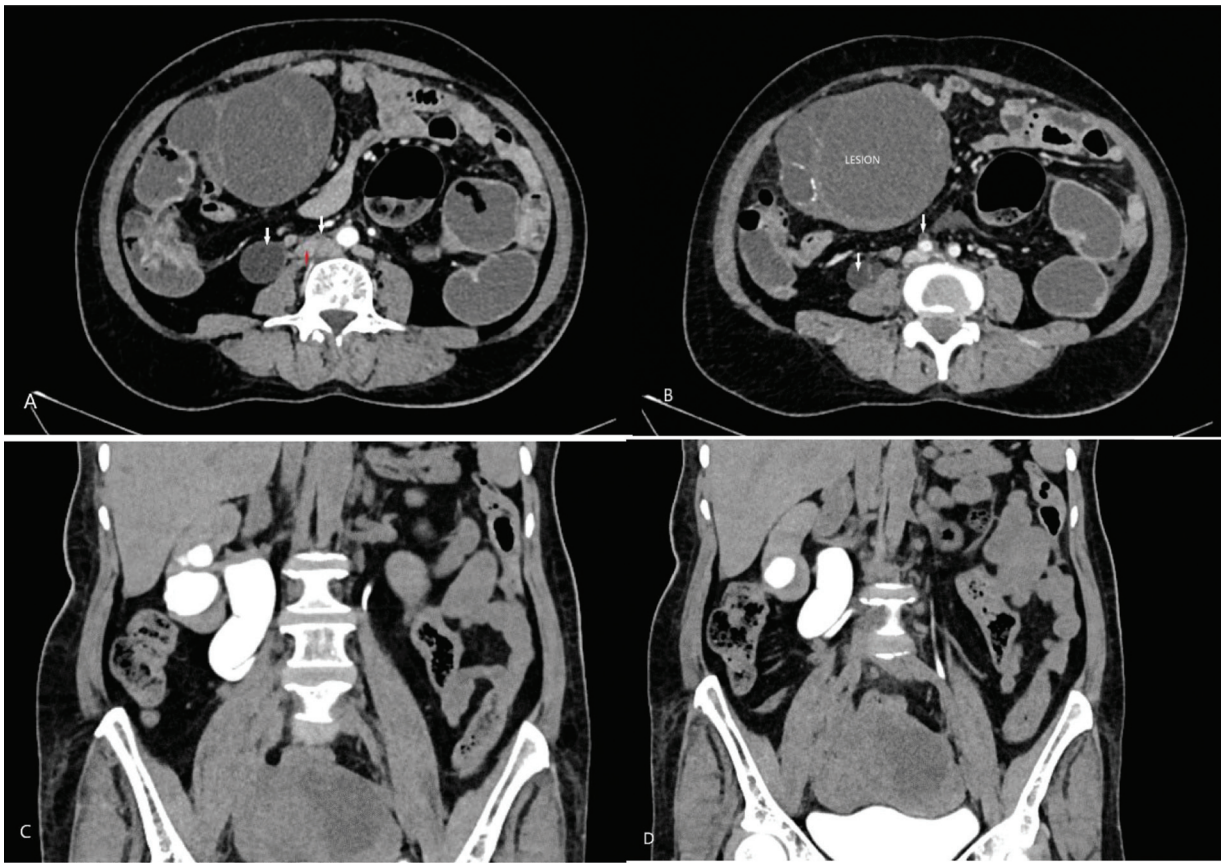

Fig. 7 (**A** and **B**) Axial postintravenous contrast computed tomography (CT) image (venous phase) showing right moderate hydroureteronephrosis with the ureter (white arrows) coursing posterior to the inferior vena cava (IVC) (red arrow). Also noted is a multiloculated right ovarian cystic neoplasm. (**C** and **D**) Coronal reformatted, delayed phase CT image showing right hydroureteronephrosis secondary to retrocaval course of ureter—J-shaped ureter.

to right-sided heart disease and sinusoidal obstruction syndrome.[17]

Primary Neoplasm of IVC

Leiomyosarcoma is a rare tumor arising from the smooth muscle cells and is the most common tumor arising from inferior vena. Upper segment involvement includes from the hepatic vein to the right atrium (24% of cases), middle segment extends from the hepatic to renal veins (42%), and lower segment involvement includes the infrarenal part of IVC (34%) (►**Fig. 12**).[18] Three main growth patterns are seen: extraluminal (62% of cases),

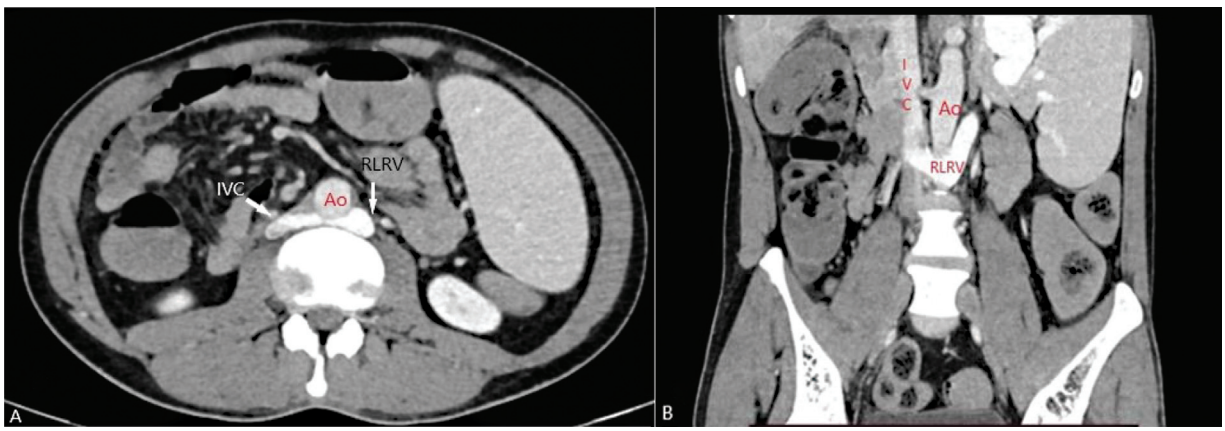

Fig. 8 (**A**) Axial postintravenous contrast computed tomography (CT) image (venous phase) showing the RLRV coursing left and posterolateral to the Ao and draining into the IVC. (**B**) Coronal reformatted, intravenous contrast-enhanced CT image (venous phase),

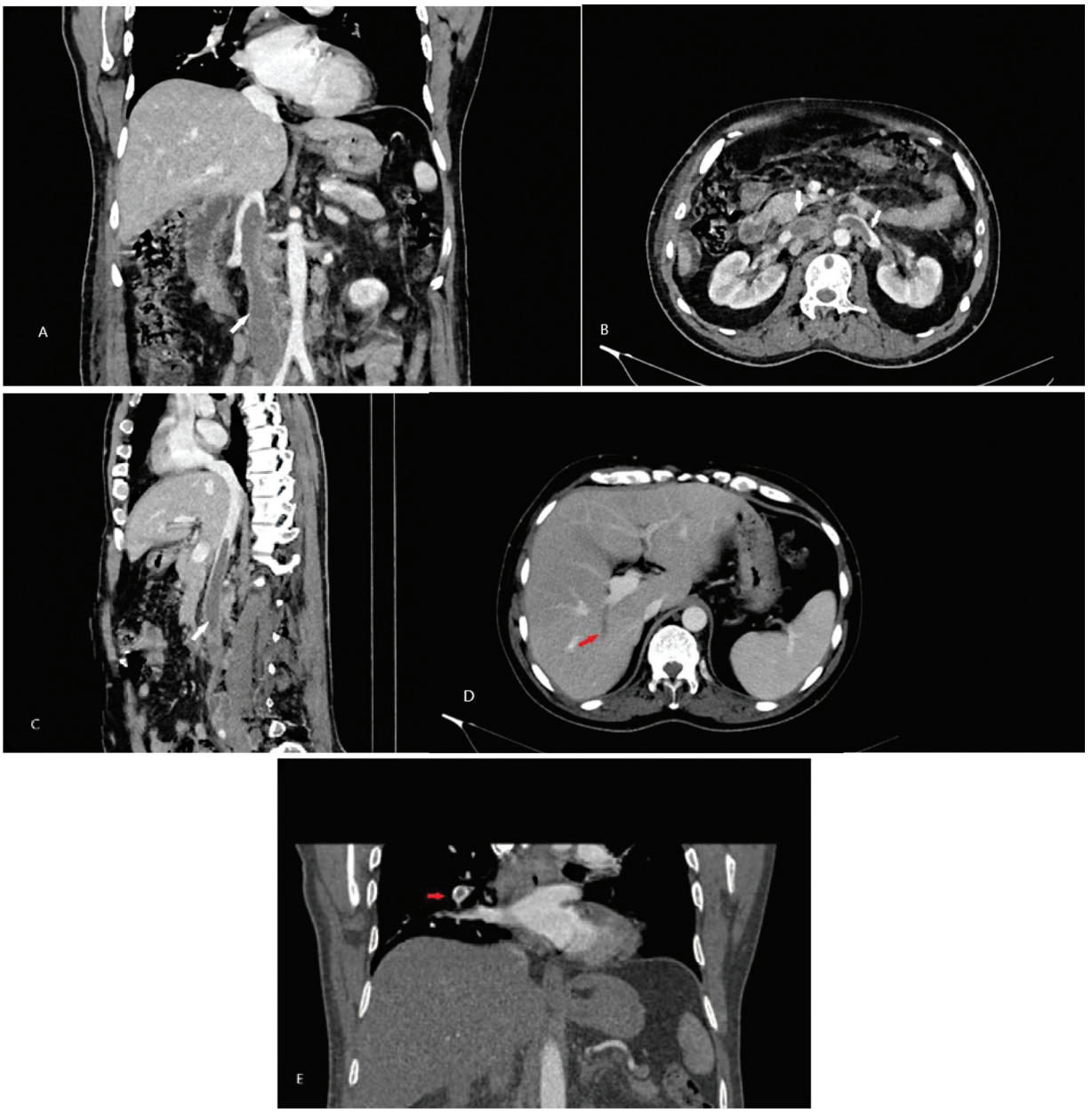

Fig. 9 (**A**) Axial postintravenous contrast computed tomography (CT) image (venous phase) and (**B**) sagittal and (**C**) coronal reformatted, intravenous contrast-enhanced CT image (venous phase) shows low attenuation nonenhancing filling defect within the inferior vena cava (IVC) and left renal veins (white arrows) consistent with bland thrombus. Enlarged necrotic retroperitoneal lymph nodes noted (red arrows). (**D**) Axial postintravenous contrast CT image (venous phase) shows low attenuation nonenhancing filling defect within the posterior segmental branch of right portal vein (white arrow). (**E**) Coronal reformatted intravenous contrast-enhanced image (venous phase) shows low attenuation central nonenhancing filling defect within the segmental branch of right descending pulmonary artery (red arrow)—polo mint sign.

intraluminal (5%), and combined extra- and intraluminal (33%).[19]

Retrograde Opacification of IVC

Retrograde opacification of IVC is linked with right-sided heart disease such as right ventricular systolic dysfunction, pulmonary hypertension, and tricuspid regurgitation (►**Fig. 13**). At low injection rates the specificity of this sign in CT is high, but the sensitivity is low. The usefulness of this classic sign decreases further with high injection rates. This fact should be kept in centers using high injection rates.[20]

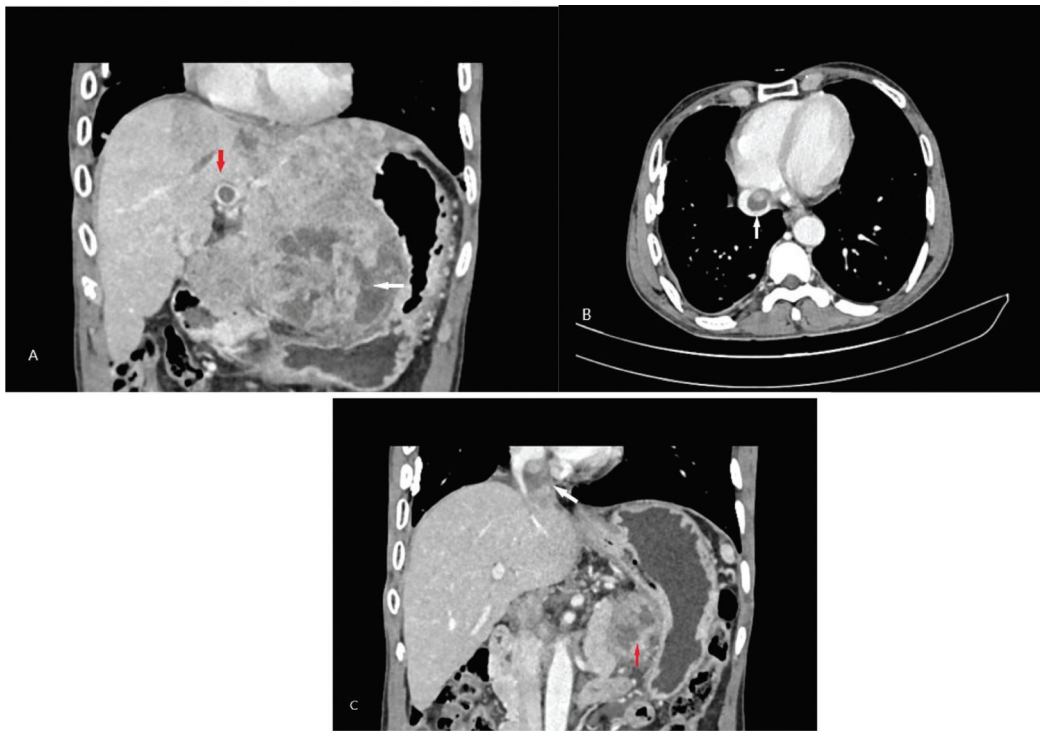

Fig. 10 (**A**) Coronal reformatted, intravenous contrast-enhanced computed tomography (CT) image (venous phase) shows heterogeneously enhancing large exophytic mass (white arrow) arising from the left lobe of liver. Also, low attenuation filling defect noted within the portal vein (red arrow). (**B**) Axial and (**C**) coronal reformatted postintravenous contrast CT image (venous phase) shows contrast enhancing tumor thrombus (white arrow) filling the lumen of inferior vena cava. Exophytic component (red arrow) of the liver mass seen.

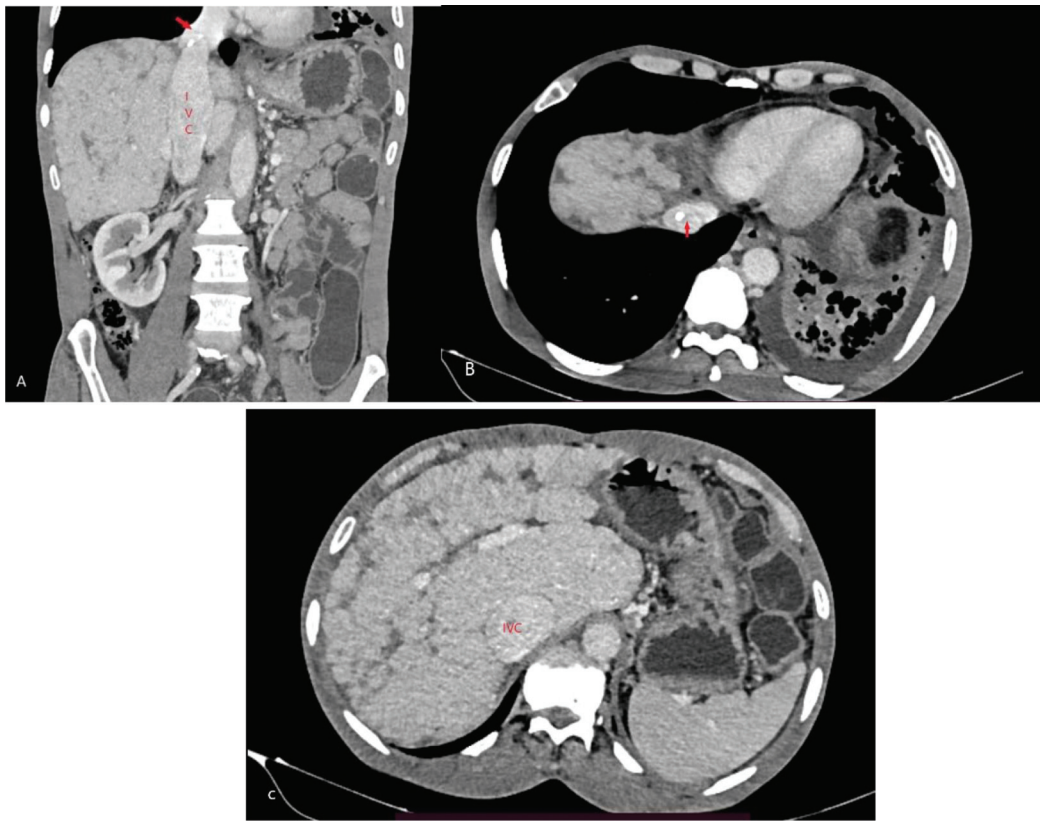

Fig. 11 (**A** and **B**) Coronal reformatted and axial, intravenous contrast-enhanced computed tomography (CT) image (venous phase) shows linear filling defect in the suprahepatic portion of the inferior vena cava with foci of calcification and mild luminal narrowing at above-mentioned site (red arrow). (**C**) Axial intravenous contrast-enhanced CT image showing the dilated intrahepatic portion of the inferior vena cava and heterogeneous enhancement of the liver-nutmeg appearance.

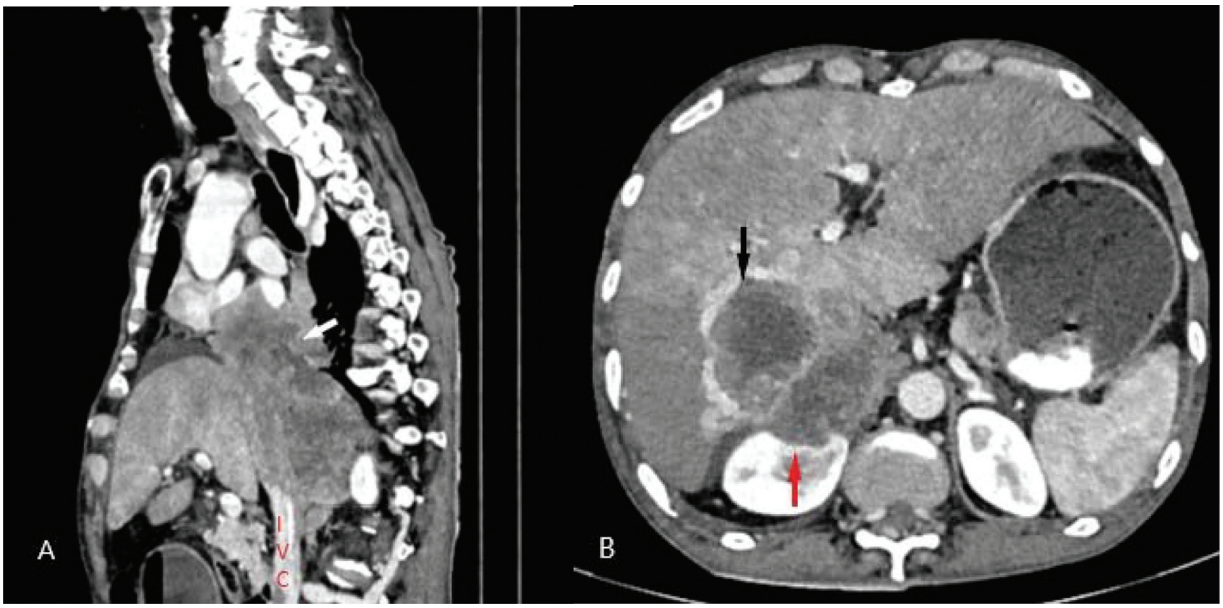

Fig. 12 (**A**) Sagittal reformatted and (**B**) Axial postintravenous contrast computed tomography (CT) image (venous phase) shows a large, heterogeneously enhanced, hypoattenuation mass causing dilatation and expansion of the inferior vena cava. The tumor extends into the right atrium (white arrow), infiltrating the liver (black arrow) and right kidney (red arrow). IVC, inferior vena cava.

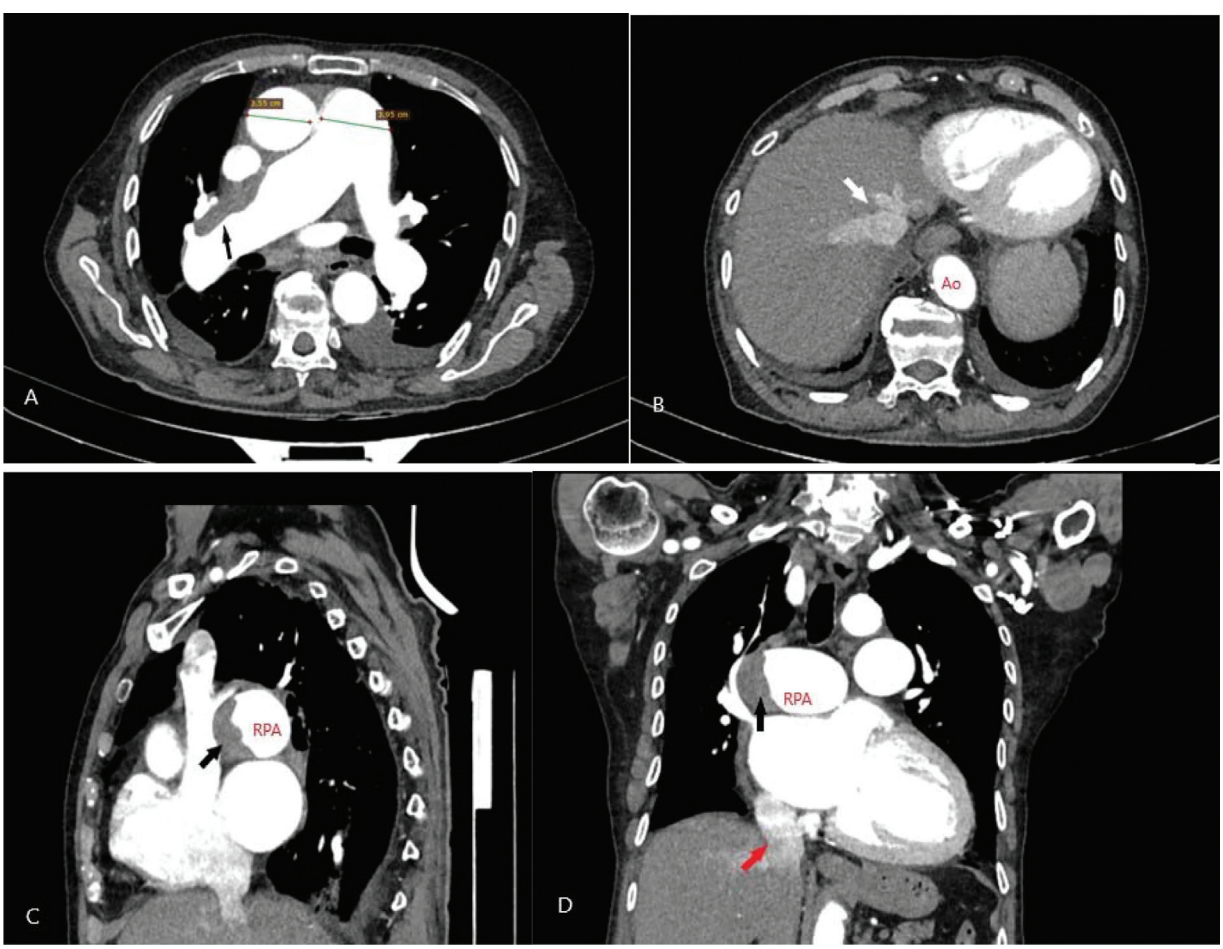

Fig. 13 (**A**) Axial intravenous contrast-enhanced computed tomography (CT) image (arterial phase) shows reversal of aortopulmonary ratio. Eccentric contrast filling defect (black arrow) suggestive of thrombus noted involving the right main pulmonary artery. (**B**) Axial intravenous contrast-enhanced CT image (arterial phase) shows early contrast opacification of the hepatic veins and inferior vena cava (IVC) (white arrow) in the arterial phase noted. (**C**) Sagittal and (**D**) coronal reformatted postintravenous contrast CT image (arterial phase) shows partial thrombosis of the right main pulmonary artery (black arrow). Early filling of the IVC and hepatic veins (red arrow) is seen. Ao, abdominal aorta; RPA, right pulmonary artery.

Funding
None.

Conflict of Interest
None declared.

References

1 Singh I, Pal GP. Human Embryology. 8th ed. India: MacMillan Publishers Limited; 2007:211–214
2 Morgan G, Superina R. Congenital absence of the portal vein: two cases and a proposed classification system for portasystemic vascular anomalies. J Pediatr Surg 1994;29(09):1239–1241
3 Frank JL, Poole CA, Rosas G. Horseshoe lung: clinical, pathologic, and radiologic features and a new plain film finding. AJR Am J Roentgenol 1986;146(02):217–226
4 Gao YA, Burrows PE, Benson LN, Rabinovitch M, Freedom RM. Scimitar syndrome in infancy. J Am Coll Cardiol 1993;22(03):873–882
5 Matsuoka T, Kimura F, Sugiyama K, Nagata N, Takatani O. Anomalous inferior vena cava with azygos continuation, dysgenesis of lung, and clinically suspected absence of left pericardium. Chest 1990;97(03):747–749
6 Petersen RW. Intrahepatic interruption of the inferior vena cava with azygos continuation (persistent right cardinal vein). Radiology 1965;84(02):304–307
7 Mathews R, Smith PA, Fishman EK, Marshall FF. Anomalies of the inferior vena cava and renal veins: embryologic and surgical considerations. Urology 1999;53(05):873–880
8 Bass JE, Redwine MD, Kramer LA, Huynh PT, Harris JH Jr. Spectrum of congenital anomalies of the inferior vena cava: cross-sectional imaging findings. Radiographics 2000;20(03):639–652
9 Nam JK, Park SW, Lee SD, Chung MK. The clinical significance of a retroaortic left renal vein. Korean J Urol 2010;51(04):276–280
10 Karaman B, Koplay M, Özturk E, et al. Retroaortic left renal vein: multidetector computed tomography angiography findings and its clinical importance. Acta Radiol 2007;48(03):355–360
11 Lesma A, Bocciardi A, Rigatti P. Circumcaval ureter: embryology. Eur Urol Suppl 2006;5(05):444–448
12 Tembely A, Diarra A, Berthé H, Diakité M, Ouattara K. Uretere Retrocave: Deux Nouvelles Observations à L'hopital Du Point G A Bamako. Afr J Urol 2014;20(02):104–107
13 Thomas TV. Surgical implications of retroaortic left renal vein. Arch Surg 1970;100(06):738–740
14 Cuéllar i Calàbria H, Quiroga Gómez S, Sebastià Cerqueda C, Boyé de la Presa R, Miranda A, Àlvarez-Castells A. Nutcracker or left renal vein compression phenomenon: multidetector computed tomography findings and clinical significance. Eur Radiol 2005;15 (08):1745–1751
15 Sheth S, Fishman EK. Imaging of the inferior vena cava with MDCT. AJR Am J Roentgenol 2007;189(05):1243–1251
16 Smillie RP, Shetty M, Boyer AC, Madrazo B, Jafri SZ. Imaging evaluation of the inferior vena cava. Radiographics 2015;35 (02):578–592
17 DeLeve LD, Valla D-C, Garcia-Tsao GAmerican Association for the Study Liver Diseases. Vascular disorders of the liver. Hepatology 2009;49(05):1729–1764
18 Ceyhan M, Danaci M, Elmali M, Ozmen Z. Leiomyosarcoma of the inferior vena cava. Diagn Interv Radiol 2007;13(03): 140–143
19 Hartman DS, Hayes WS, Choyke PL, Tibbetts GP. From the archives of the AFIP. Leiomyosarcoma of the retroperitoneum and inferior vena cava: radiologic-pathologic correlation. Radiographics 1992; 12(06):1203–1220
20 Yeh BM, Kurzman P, Foster E, Qayyum A, Joe B, Coakley F. Clinical relevance of retrograde inferior vena cava or hepatic vein opacification during contrast-enhanced CT. AJR Am J Roentgenol 2004; 183(05):1227–1232

